

## Local bifurcation and interior crisis in a ring cavity system of spatially distributed optical nonlinear elements

This article has been downloaded from IOPscience. Please scroll down to see the full text article.

1994 J. Phys. A: Math. Gen. 27 3051

(<http://iopscience.iop.org/0305-4470/27/9/019>)

View [the table of contents for this issue](#), or go to the [journal homepage](#) for more

Download details:

IP Address: 171.66.16.68

The article was downloaded on 01/06/2010 at 23:58

Please note that [terms and conditions apply](#).

## Local bifurcation and interior crisis in a ring cavity system of spatially distributed optical nonlinear elements

Tong Kun Lim, Young Hun Yu and Joong Mok Park

Department of Physics, Korea University, Seoul, Korea

Received 13 April 1993, in final form 11 October 1993

**Abstract.** A ring cavity system showing chaotic behaviour is constructed with three hybrid Michelson interferometers unidirectionally coupled to one another. This is for the first step in the study of spatiotemporal chaos. This system exhibits spatiotemporal chaotic behaviours of the type described by Ikeda and Otsuka. It shows local bifurcation phenomena, such as pitchfork bifurcation and saddle-node bifurcation, as well as Hopf bifurcation. Also, an isola-type solution mode was found for the system and a target-shooting method was used to make the system reach this isola mode. We have observed an interior crisis in this isola mode when there is a delay in the feedback signal to the nonlinear elements. Both the computer simulations and experimental work were performed to investigate these phenomena.

### 1. Introduction

There have been many theoretical as well as experimental investigations on chaotic phenomena such as pitchfork bifurcation [4], saddle-node bifurcation [5], transcritical bifurcation, Hopf bifurcation [8] and isola-type phenomena [6]. Recently, Otsuka and Ikeda proposed a model system which can be used as a first step in studying these complicated spatiotemporal behaviours [1, 2]. Their system is basically a ring cavity system composed of many nonlinear elements spatially distributed and coupled to one another by feedbacking the output signal of each element to the next. Although there have been many theoretical works on this type of system, few experimental studies have been performed on it. This system is also an interesting system for a possible application as a logic or memory device [12, 13]. In this paper we report on some results of an experimental study of chaotic phenomena performed with this system. For this purpose we have constructed an Ikeda–Otsuka-type ring cavity system with three hybrid Michelson interferometers as nonlinear elements. The output of each element is fed back to the next one on the right-hand side and the output of the last one is fed back to the first one, thereby forming a ring cavity. This system shows that it has two spatial modes of solution, one of them is an isola mode and the other is its symmetric mode. We find by computer simulation as well as by experimental study that the isola mode is formed through saddle-node bifurcation and the symmetric model through Hopf bifurcation. The effect of delay time in the feedback signal on the behaviour of the isola mode is also studied, as was done previously by Chern and McIver [6]. It is found that delays in the feedback signals make this ring cavity system undergo an interior crisis as well as a period-doubling process.

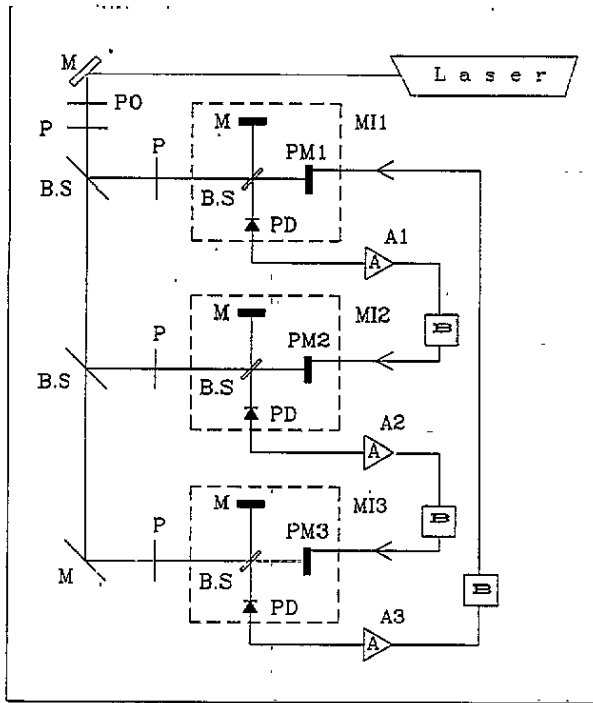


Figure 1. A schematic diagram of the experimental set-up. PD, photodiode; A, amplifier; MI*i*, *i*th Michelson interferometer; B, buffer for the delay feedback signal; M, mirror; PM, piezo-ceramic buzzer and mirror; BS, beam splitter.

## 2. Theoretical model and computer study

### 2.1. Model

The schematic diagram of our experimental system is shown in figure 1. Each nonlinear element is basically a Michelson interferometer, the output of which is fed back to a pZT that drives the mirror in one arm of the next lowest interferometer, and the output of the lowest one to that of the first one. In this way the system forms a ring cavity configuration.

When there is a delay time  $T$  in the feedback signal from the  $k$ th element to the  $(k+1)$ th element, the difference differential equations governing the spatially distributed ring cavity system in figure 1 are as follows:

$$\tau \frac{d\phi_{k+1}(t)}{dt} + \phi_{k+1}(t) = f(\phi_k) = I_0 [1 + V_k \cos(\phi_k(t-T) + \phi_{k0})]$$

$$(k = 1, 2, 3, \dots, N). \quad (1)$$

Here  $k$  denotes the spatial position of the interferometers,  $\tau$  is the response time of each interferometer and  $V_k$  is the visibility of the  $k$ th interferometer,  $\phi_{k0}$  is the phase difference due to the unequal lengths of beam paths in the  $k$ th interferometer when there is no feedback, and  $\phi_k$  is the phase difference when there is feedback to the interferometer.

## 2.2. Bifurcations of the stationary solution

The stationary solution  $\phi_{k+1}^*$  of the  $(k+1)$ th element can be obtained from equation (1) as in [1,2] using periodic boundary conditions:

$$\phi_{k+1}^* = f(\phi_k^*) \quad \phi_{N+1}^* = \phi_1^* \quad (k=1, 2, 3, \dots, N) \quad (2)$$

$$\phi_k^* = f(\phi_{k-1}^*) = f(f(\dots(\phi_k^*)\dots)) = f^{(N)}(\phi_k^*) \quad (k=1, 2, 3, \dots, N). \quad (3)$$

Since  $f(\phi_k^*)$  is a nonlinear function, there can be many possible values of  $\phi_k^*$  for each  $k$ th interferometer. The set of values  $\{\phi_k^*\} = \{\phi_1^*, \phi_2^*, \phi_3^*, \dots, \phi_N^*\}$  form spatial patterns, i.e. spatial modes.

In this work we used a system of three nonlinear elements ( $N=3$ ). The stationary solutions  $\phi_k^*$  obtained from computer simulation as a function of input intensity  $I_0$  are shown in figure 2. We have kept the visibility  $V_k$  at 0.7 and the initial phase difference  $\phi_{k0}$  at 0 or  $\pi$  for all elements. The laser input intensity  $I_0$  is used as a control parameter (or bifurcation parameter) in a range from 0 to 5.

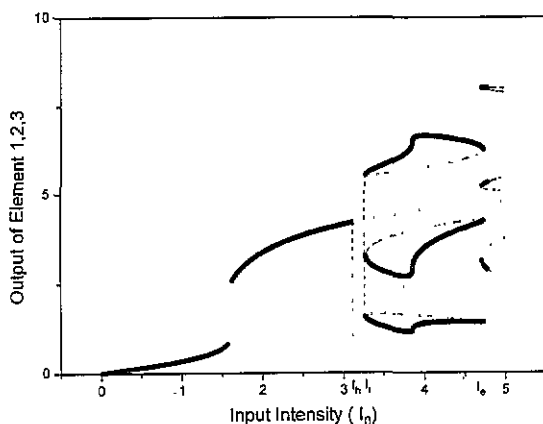


Figure 2. The stationary solution for the output of the system with three elements (full line, stable solution; dotted line, unstable solution).

The full line in figure 2 depicts the temporally stable stationary solution, and the dotted line depicts the temporally unstable solution determined by linear stability analysis. When the control parameter is between 0 and 3.21 ( $=I_h$  in figure 2) the outputs of all three elements are same and are stable; however, the outputs are dynamically unstable in a small range of  $I_0$  between 3.21 ( $=I_h$ ) and 3.28 ( $=I_i$ ). For higher values of  $I_0$  between 3.28 ( $=I_i$ ) and 4.72 ( $=I_e$ )  $\phi_k^*$  has two spatial modes. One mode is a symmetric mode in which the outputs of all three elements are same but unstable. This mode is depicted in figure 2 as a single dotted line extending from single-valued solution curves of lower  $I_0$ . In the other mode of  $\phi_k^*$  the outputs of all three elements are different from one another and each one of them forms a separate closed curve in the  $\phi_k^*$  versus  $I_0$  diagram, as shown in figure 2. This mode is called isola [3, 6, 7, 11]. In this mode we find that the outputs always keep their cyclic relation in a certain direction, as was discussed by Chern and McIver [6]. If one element has its output value corresponding to that in the lowest isola, the next one in the anticlockwise direction, for example, has its output value for that of the middle isola, and the last one that of the highest isola. From the linear stability analysis we have three eigenvalues  $\lambda$  in the short delay

limit [1, 2]:

$$\begin{aligned}\lambda_1 &= -1 - S \\ \lambda_2 &= -1 + \frac{S}{2} + i\frac{\sqrt{3}}{2}S \\ \lambda_3 &= -1 + \frac{S}{2} - i\frac{\sqrt{3}}{2}S\end{aligned}\tag{4a}$$

when  $\sigma < 0$  and

$$\begin{aligned}\lambda_1 &= -1 + S \\ \lambda_2 &= -1 - \frac{S}{2} + i\frac{\sqrt{3}}{2}S \\ \lambda_3 &= -1 - \frac{S}{2} - i\frac{\sqrt{3}}{2}S\end{aligned}\tag{4b}$$

when  $\sigma > 0$ .

Where

$$\sigma \equiv \prod_{k=1}^N f(\phi_k^*)$$

and  $S \equiv \sqrt[3]{|\sigma|}$ .

In the symmetric mode of solution in the range  $I_0$  larger than  $I_h$  ( $=3.21$ ) the values of  $\lambda_2$  and  $\lambda_3$  are pure imaginary and complex conjugate to each other for the stationary solutions, while the real part of  $\lambda_1$  is negative for them. This is the situation when the system undergoes a Hopf bifurcation. Figure 3 shows a Hopf-bifurcated signal obtained with  $I_0$  at 3.6, which is larger than the Hopf bifurcation point  $I_h$ . The output of each element is in fact sinusoidal. The phase difference in between the neighbouring elements  $\phi$  is  $2\pi/3$  due to the boundary condition.

The isola shown in figure 2 is created through a saddle-node (tangent) bifurcation. In our system the starting point and the ending point of  $I_0$  for the isola are 3.28 ( $I_i$ ) and 4.72 ( $I_e$ ), respectively. At these extreme points the triple iteration  $f(f(f(\phi_k^*)))$  of the nonlinear function  $f(\phi_k)$  has a tangent line whose slope is 1. The real parts of the eigenvalues  $\lambda_2$  and  $\lambda_3$  have the same negative value, and the value of  $\lambda_1$  is zero at the starting point  $I_i$  as well as at the ending point  $I_e$ . There are two fixed points for a given value of  $I_0$  in the isola. When  $\sigma < 1$ , all three eigenvalues have negative real parts and the fixed parts are nodal points. When  $\sigma > 1$ , two eigenvalues have negative real parts whereas one has a positive value so it is a saddle point. Since the isola solutions are separated from the symmetric solution, as is clear in figure 2, they cannot be reached by gradually increasing the magnitude of the control parameter  $I_0$  from zero. However, they can be reached by a target-shooting method, i.e. by choosing the initial values of the transit signal from the attracting basin of the isola. When this method is applied, the output values of the interferometer automatically go to the nodal points of the isola since the nodal points are the only temporally stable points in the isola.

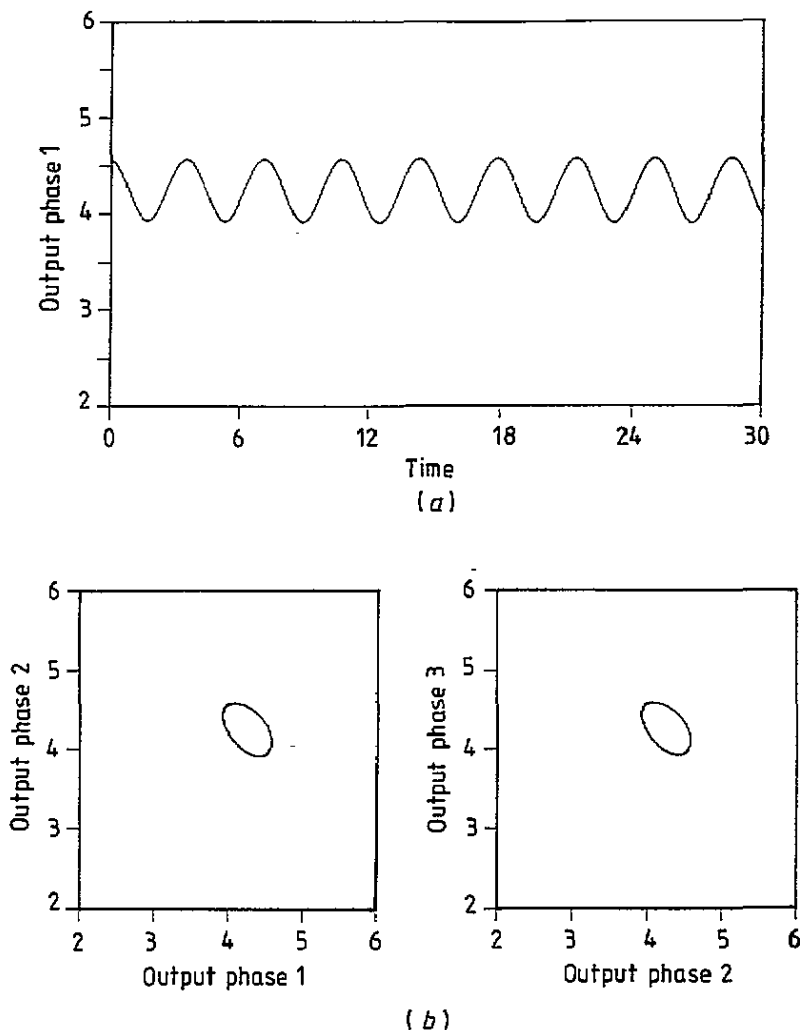


Figure 3. The Hopf bifurcation at  $I_0=3.6$  by computer simulation. (a)  $\phi_1$  after Hopf bifurcation. (b)  $\phi_{k+1}$  versus  $\phi_k$ .

### 2.3. Interior crisis

When the feedback signals are delayed in time, the stable solutions (nodal point) of the isola become unstable and turn chaotic through a period-doubling process. The basin of this chaotic regime is enlarged as the delay time becomes larger, while the unstable solutions do not change their values. Eventually the basin of this chaotic range touches the unstable points, and the interior crisis takes place with a sudden expansion of the attracting basin from the isola region to the full region which contains all three isola regions, thus developing a full-range chaos [6, 8–10]. Figure 4 shows this colliding phenomena (interior crisis) in the region  $I_0 > 4.07$  when the normalized delay time ( $T/\tau$ ) is 1. Note that initially forbidden regions between the isola curves are filled with chaotic solutions after the interior crisis takes place. We also have other expanded chaotic regimes of nodal points in the middle of the isola ( $I_{oc} < I_0 < I_{cf}$ ), but they do not

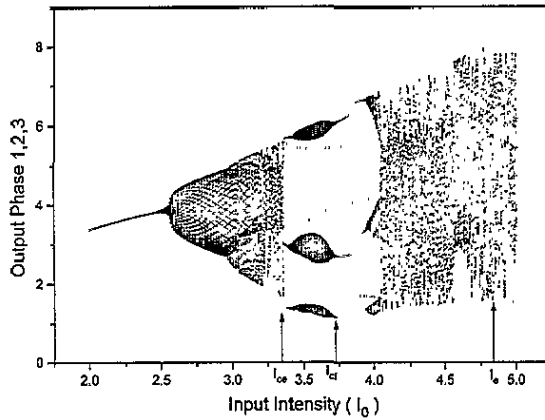
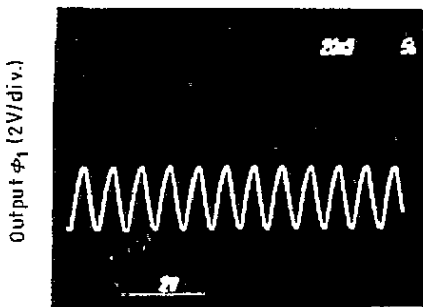
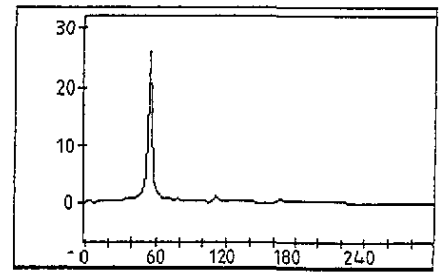


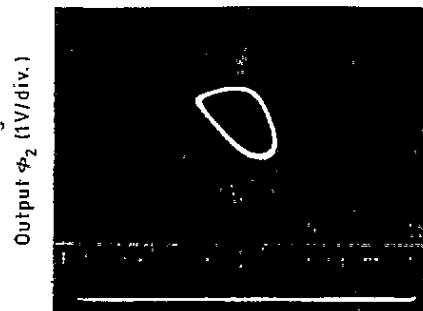
Figure 4. The output solution when the system shows the interior crisis of isola. The normalized delay time ( $T/\tau$ ) is 1.0 (computer simulation results). The dotted line is the unstable solution branch.



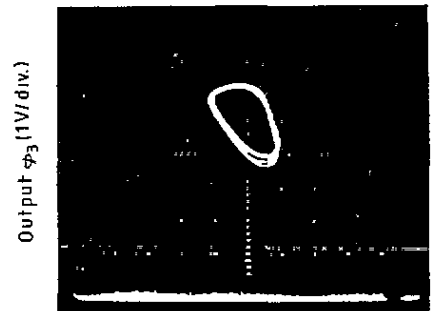
(a) Time (20 ms/div.)



(b) The power spectrum of  $\phi_1$



(c) Output  $\phi_1$  (1V/div.)



Output  $\phi_2$  (1V/div.)

Figure 5. The Hopf bifurcation of symmetric solution. (a) The time behaviour of the Hopf bifurcated signal. (b) The power spectrum of the Hopf bifurcated signal. (c)  $\phi_{k+1}$  versus  $\phi_k$ .

collide with the saddlepoint branch even with a very large delay time, and we have isola-type chaos in this region [6].

### 3. Experimental results

As is shown in figure 1 our experimental system is basically a ring cavity system made of three nonlinear elements coupled to each other with delayed feedback. Each nonlinear element is a hybrid Michelson interferometer. The output of each interferometer is detected by a photodiode, and the signal is then amplified and fed back to a buzzer (SAT 1050, Sonitron Co.) mounted on a mirror on one arm of the next interferometer, thereby varying the output of the interferometer nonlinearly. The delay time of the feed-back signal is varied by controlling the transit time of the transmitting signal in the buffer. The light source is a 5 mW He-Ne laser (Uniphase Co.). We kept the visibility  $V_k$  at  $0.7 \pm 0.03$  and the initial phase difference  $\phi_{k0}$  at  $\pi \pm 0.05$  for all elements, and the response time  $\tau$  of each element was measured to be  $4.08 \pm 0.08$  ms.

Figure 5 shows the output of one of the interferometers, when  $I_0$  is larger than  $I_h$  ( $=3.21$ ). It is a typical signal which a system gives after Hopf bifurcation. It is very similar to that of figure 3. The Hopf bifurcated outputs are found to be sinusoidal and to have  $2\pi/3$  phase difference between neighbouring elements as shown in figures 5(c) and 5(d). The spectrum of  $\phi_k(t)$  shown in figure 5(b) tells us that  $\phi_k(t)$  has a reasonably good sinusoidal functional form.

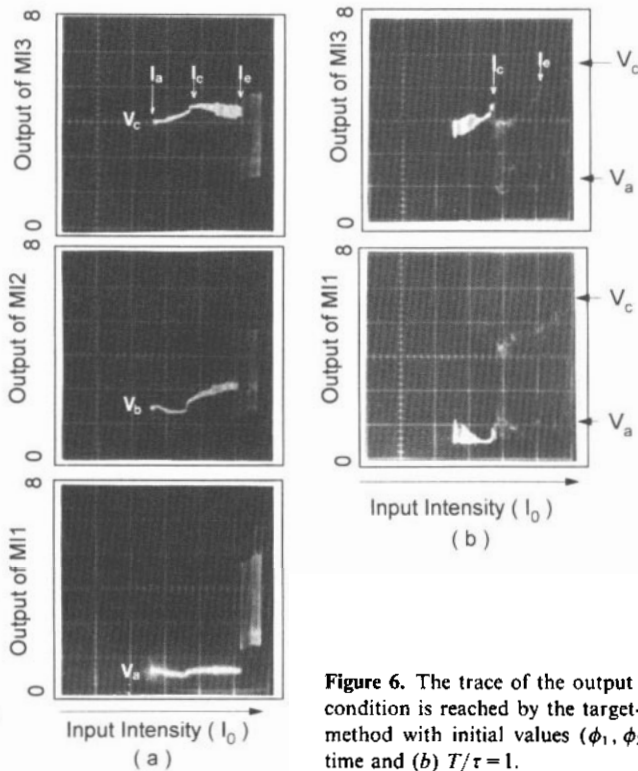


**Figure 6.** The trace of the output in the system in the isola region. This condition is reached by the target-shooting method. The target-shooting method with initial values  $(\phi_1, \phi_2, \phi_3) = (1.4, 3.1, 6.0)$  for (a) no delay time and (b)  $T/\tau = 1$ .



Figures 6(a) and 6(b) show the tracing of the outputs obtained by the target-shooting method when the system is in the isola mode. In figure 6(a), which shows the case when the system has no delay in the feedback, the output values  $V_a$ ,  $V_b$  and  $V_c$  correspond to the stable solutions of the lowest, middle and uppermost isola curves, respectively, in figure 2. When there is a delay time in the feedback signal, the output of each element becomes chaotic as the delay times increase. When the normalized delay time is increased up to 1, the chaotic basins finally touch the saddle-node points in the range of  $I_0$  from  $I_c$  to  $I_e$ , and this chaotic region expands to the full region  $V_a$  to  $V_c$  of the three isolas. This is direct evidence of the fact that the interior crisis has taken place. The experimental results of the crisis are similar to that of the computer simulation of figure 4.

#### 4. Conclusion

We have constructed a ring cavity system composed of nonlinear elements coupled to one another with a feedback signal. With this system we have investigated some local bifurcation phenomena. Two spatial modes were found to exist in this type of system, one of which is a symmetric mode of solution and the other is its isola mode. A Hopf bifurcation is observed in the symmetric mode and a saddle-node bifurcation is observed in the isola mode. Hopf bifurcation occurs when the two characteristic eigenvalues have a complex conjugate relation and the third one has a negative real part. The isolas are born through saddle-node bifurcation, and we have found that one can enter the isola region by using the target-shooting method. It has also been shown experimentally as well as by the computer simulation that the isola-type chaos is terminated by an interior crisis when the delay time in the feedback is increased.

#### References

- [1] Otsuka K and Ikeda K 1987 *Phys. Rev. Lett.* **59** 194
- [2] Otsuka K and Ikeda K 1987 *Phys. Rev. A* **39** 5209
- [3] van Heerden C 1953 *Ind. Eng. Chem.* **45** 1242
- [4] Chern J L and McIver J K 1989 *Phys. Lett.* **142A** 99
- [5] Crawford J D 1991 *Rev. Mod. Phys.* **63** 991
- [6] Chern J L and McIver J K 1991 *Phys. Lett.* **158A** 209
- [7] Guckenheimer J and Holmes P 1986 *Nonlinear Oscillations, Dynamical Systems and Bifurcations of Vector Fields* 2nd edn (Berlin: Springer) ch 3
- [8] Grebogi C et al 1983 *Physica* **7D** 181
- [9] Wang C S et al 1991 *Phys. Lett.* **152A** 21
- [10] Grebogi C et al 1982 *Phys. Rev. Lett.* **48** 1507
- [11] Kubicek M et al 1982 *J. Comput. Phys.* **40** 106
- [12] Firth W J *Phys. Rev. Lett.* **61** 329
- [13] Otsuka K 1989 *Opt. Lett.* **14** 72